Intramolecular Hydrogen Transfer as the Key Step in the Dissociation of Hydroxyl Radical Adducts of (Alkylthio)ethanol Derivatives

Christian Schöneich*,† and Krzysztof Bobrowski*,‡,§

Contribution from the Department of Pharmaceutical Chemistry, University of Kansas, Lawrence, Kansas 66045, and Radiation Laboratory, University of Notre Dame, Notre Dame, Indiana 46556

Received December 14, 1992

Abstract: The reaction of the hydroxyl radical with dimethyl sulfide (DMS), 2-(methylthio)ethanol (2-MTE), 2,2′-dihydroxydiethyl sulfide (2,2′-DHE), and 3,3′-dihydroxydipropyl sulfide (3,3′-DHP) has been investigated in H_2O and D_2O. As an initial step hydroxyl radicals add to the sulfur moiety. These hydroxyl radical adducts subsequently decay via a thioether concentration-dependent and a thioether concentration-independent pathway. The hydroxyl radical adduct of DMS dissociates into a sulfur radical cation and HO^- in the thioether concentration-independent pathway ($k_H/k_D = 2.09$), whereas a rate-limiting proton transfer from water operates in the thioether concentration-dependent mechanism ($k_H/k_D = 5.40$), as deduced from the measured solvent kinetic isotope effects. In contrast the hydroxyl radical adducts of 2-MTE and 2,2′-DHE decompose via elimination of water, formed through a rapid intramolecular hydrogen transfer from the adjacent hydroxyl groups. This mechanism leads to the formation of (alkylthio)ethoxy radicals. The latter undergo α,β-fragmentation into formaldehyde and α-thioether radicals as well as hydrogen abstraction from a δ-methylene group, analogous to a hydrogen transfer in the Barton reaction, leading to α-thioether radicals. The overall rate constants for these unimolecular reaction sequences were determined to be $k_{12,H} = (6.32 \pm 0.7) \times 10^7$ s^{-1} for 2-MTE and $k_{15,H} = (1.17 \pm 0.2) \times 10^8$ s^{-1} for 2,2′-DHE. Neither of them show an appreciable kinetic isotope effect, suggesting that the actual hydrogen transfer is not the rate-determining step in the overall process.

Introduction

Oxidation mechanisms by oxygen free radicals have been thoroughly investigated over the past years due to their general importance in many chemical and biochemical processes.[1,2] In particular the hydroxyl radical ($HO^•$) has been identified as one of the major deleterious species in the biological environment. Formation of hydroxyl radicals and their subsequent reactions with biomolecules have become the basis for explaining the pathogenesis of many cellular dysfunctions and diseases (e.g. cancer, arthritis) in the course of "oxidative stress" and aging.[1,2]

A common procedure for obtaining evidence for the participation of hydroxyl radicals in biological oxidations or oxidative processes, in general, is based on product studies. This approach has, for example, led to the identification of the involvement of hydroxyl radicals in the damage of DNA[3,4] and tRNA[5] via transition metal-catalyzed activation of oxygen in the presence of suitable metal chelators. At present, considerable research effort focuses on the therapeutic use of these DNA-damaging propensities of metal chelators. Iron–EDTA complexes, for example, are chemically bound to molecules which specifically bind to certain domains of DNA, resulting in a specific cleavage (strand breakage).[6-10]

Product studies, however, require a detailed knowledge about the underlying mechanisms and kinetics of the reaction of the hydroxyl radical with the molecule of interest.

Organic thioethers are particularly susceptible to oxidation. In many proteins, for example, methionine has been found to undergo oxidation under conditions of oxidative stress.[11] *In vitro* studies have led to the characterization of mechanisms by which various oxygen free radicals interact with organic sulfur compounds and finally lead to the formation of the observed products. The hydroxyl radical induced oxidation of dimethyl sulfide and other organic sulfides in H_2O was first studied by Asmus and co-workers.[12-16] It is now well established that addition of the hydroxyl radical to the sulfur constitutes the first step in the oxidation process.[12-14] However, the mechanisms by which these adducts decay into more stable products are still under controversial discussion. In the present study, mechanistic details of the latter processes were addressed by employing solvent kinetic isotope effects. Subsequently these data were used as a basis to explain unexpected observations during the hydroxyl radical induced oxidation of hydroxy-substituted organic sulfides. It will be shown, using nanosecond pulse radiolysis, that the reaction of the hydroxyl radical with (alkylthio)ethanol derivatives leads to products that are untypical for the reaction of $HO^•$ with both thioethers and aliphatic alcohols. The underlying mechanism

† University of Kansas.
‡ University of Notre Dame.
§ K.B. is on leave of absence from the Institute of Biochemistry and Biophysics, Polish Academy of Sciences, 02-532 Warsaw, Poland.

(1) *Oxygen Radicals in Biology and Medicine*; Simic, M. G., Taylor, K. A., Ward, J. F., von Sonntag, C., Eds.; Plenum Press: NY, 1988.
(2) *Oxygen Free Radicals in Tissue Damage*; Tarr, M., Samson, F., Eds.; Birkhäuser: Boston, 1993.
(3) Halliwell, B.; Gutteridge, J. M. C. *FEBS Lett.* **1992**, *307*, 108–112.
(4) Aruoma, O. I.; Halliwell, B.; Gajewski, E.; Dizdaroglu, M. *J. Biol. Chem.* **1989**, *264*, 20509–20512.
(5) Hüttenhofer, A.; Noller, H. F. *Proc. Natl. Acad. Sci. U.S.A.* **1992**, *89*, 7851–7855.
(6) Aiyar, J.; Danishefsky, S. J.; Crothers, D. M. *J. Am. Chem. Soc.* **1992**, *114*, 7552–7554.
(7) Ebright, Y. W.; Chen, Y.; Pendergrast, P. S.; Ebright, R. H. *Biochemistry* **1992**, *31*, 10664–10670.
(8) Schepartz, A.; Cuenoed, B. *J. Am. Chem. Soc.* **1990**, *112*, 3247–3249.
(9) Hoyer, D.; Cho, H.; Schultz, P. G. *J. Am. Chem. Soc.* **1990**, *112*, 3249–3250.
(10) Rana, T. M.; Meares, C. F. *J. Am. Chem. Soc.* **1990**, *112*, 2457–2458.
(11) (a) Moreno, J. J.; Pryor, W. A. *Chem. Res. Toxicol.* **1992**, *5*, 425–431. (b) Evans, M. D.; Pryor, W. A. *Chem. Res. Toxicol.* **1992**, *5*, 654–660. (c) Hall, P. K.; Roberts, R. C. *Biochim. Biophys. Acta* **1992**, *1121*, 325–330. (d) Maier, K. L.; Matejkova, E.; Hinze, H.; Leuschel, L.; Weber, H.; Beck-Speier, I. *FEBS Lett.* **1989**, *250*, 221–226. (e) Brot, N.; Weissbach, H. *Arch. Biochem. Biophys.* **1983**, *223*, 271–281.
(12) Bonifačić, M.; Möckel, H.; Asmus, K.-D. *J. Chem. Soc., Perkin Trans. 2* **1975**, 675–685.
(13) Janata, E.; Veltwisch, D.; Asmus, K.-D. *Radiat. Phys. Chem.* **1980**, *16*, 43–49.
(14) Asmus, K.-D.; Bahnemann, D.; Bonifačić, M.; Gillis, H. A. *Faraday Discuss. Chem. Soc.* **1978**, *63*, 213–225.
(15) Mönig, J.; Goslich, R.; Asmus, K.-D. *Ber. Bunsen-Ges. Phys. Chem.* **1986**, *90*, 115–121.
(16) Asmus, K.-D. *Acc. Chem. Res.* **1979**, *12*, 436–442.

0002-7863/93/1515-6538$04.00/0

involves a simultaneous interaction of the hydroxyl radical with the thioether and the alcohol group in a cyclic transition state.

The results provide an example showing that mechanistic information available for the reaction of the hydroxyl radical with one particular functional group cannot simply be generalized but must be carefully examined with respect to possible neighboring group effects on reaction kinetics and product distribution.

Experimental Section

Materials. The sulfur compounds dimethyl sulfide (DMS), 2-(methylthio)ethanol (2-MTE), 2,2′-dihydroxydiethyl sulfide (2,2′-DHE), and 3,3′-dihydroxydipropyl sulfide (3,3′-DHP) were purchased from Aldrich Chemical Company (St. Louis, MO). In order to remove trace amounts of thiols, DMS was extracted repeatedly with alkaline water (pH 13–14) followed by washing with neutral water and distillation. 2-MTE, 2,2′-DHE, and 3,3′-DHP were of highest commercially available purity and used without further purification. (2,4-Dinitrophenyl)hydrazine was from Eastman Chemicals. Formaldehyde was purchased from Fisher Chemical (Fair Lawn, NJ) as a 37% (w/w) aqueous solution. HPLC grade acetonitrile was supplied by Fisher Chemical (Fair Lawn, NJ). Water was purified by a Millipore Milli-Q system. Deuterium oxide (D_2O) was supplied by DOE, Savannah River Site.

Solutions. All solutions were made up freshly and purged for at least 30 min per 100 mL with N_2O prior to the experiment. The respective pH values were measured using an Orion glassy and calomel pH electrode coupled to an Orion pH meter 811 and, if necessary, adjusted with small concentrations of $HClO_4$ or NaOH. Reactions in D_2O were carried out at pD values between 7.0 and 7.6 (pD = pH + 0.4). Therefore any trace of H^+ or HO^- introduced by adjusting the pD with $HClO_4$ or NaOH was negligible. Similarly, the introduction of protons into D_2O by H/D exchange of 2-MTE and 2,2′-DHE can be considered to be negligible. The maximum used concentrations of the latter alcohols in D_2O were 0.1 M (with ρ_{D_2O} = 1.1 g/mL the concentration of D_2O is 55.0 M). All solutions were kept at 25 ± 1 °C.

Pulse Radiolysis. All pulse radiolysis experiments were performed by applying 5-ns pulses of high-energy electrons from the Notre Dame 7 MeV ARCO LP-7 linear accelerator. Absorbed doses were in the order of 4–6 Gy (1 Gy = 1 J/kg). A description of the pulse radiolysis setup and data collection is reported elsewhere.[17] The experiments were carried out with a continuous flow of the sample solution.

γ-Radiolysis. The γ-radiolysis experiments were carried out in the field of a 24 000-Ci ^{60}Co source (Model 109/68 ^{60}Co irradiator, JL Shepherd & Associates, Glendale, CA). The employed dose rate was 99.6 Gy/min as determined by Fricke dosimetry.[18]

HPLC. HPLC analysis was carried out using a Hewlett-Packard 1090 chromatograph equipped with a diode array UV/vis detector.

Analysis of Formaldehyde. The analysis of formaldehyde was carried out by derivatization with (2,4-dinitrophenyl)hydrazine followed by HPLC analysis. A 1-mL aliquot of an irradiated solution was reacted for 10 min with 1 mL of a solution of 10^{-2} M (2,4-dinitrophenyl)hydrazine in 10^{-2} M HCl. Subsequently the reaction mixture was extracted with 1 mL of an *n*-hexane/CH_2Cl_2 (80:20, v/v) mixture by stirring for 5 min. The organic layer, containing the hydrazone, was separated from the aqueous phase, and a 5-μL aliquot was injected onto an HPLC column (SGE Hypersil C18, 5 μm, 250 × 4.6 mm) which was eluted isocratically with acetonitrile/water, 60:40 (v/v), at a flow rate of 1 mL/min. Identification of the hydrazones was achieved by UV detection at 345 nm. Under the HPLC conditions the formaldehyde hydrazone eluted with t_R = 3.9 min. Quantification was achieved by conducting the same procedure with authentic formaldehyde samples.

Results

Pulse Radiolysis. Pulse irradiation of water leads to the formation of the highly reactive species shown in reaction 1.[19] In

$$H_2O \rightarrow e_{aq}^-, HO^\bullet, H^\bullet \qquad (1)$$

N_2O-saturated aqueous solutions ($[N_2O]_{sat} \approx 2.0 \times 10^{-2}$ M[19]) the hydrated electrons, e_{aq}^-, are converted into hydroxyl radicals

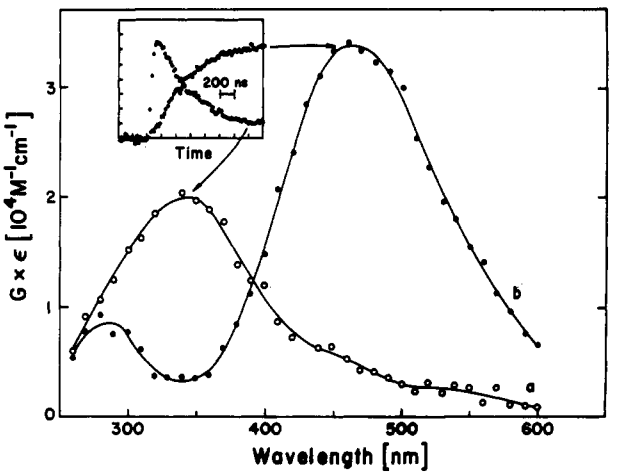

Figure 1. Transient absorption spectra observed (a) 120 ns and (b) 1.4 μs after pulse irradiation of a 2.0 mM solution of DMS in H_2O saturated with N_2O at pH 6.7. Inset: Absorption vs time profiles of the decay of **1a** (340 nm) and the formation of **2a** (465 nm).

according to reaction 2 ($k_2 = 9.1 \times 10^9$ M^{-1} s^{-1} [17]). In the presence

$$e_{aq}^- + N_2O \rightarrow HO^\bullet + N_2 + HO^- \qquad (2)$$

of N_2O the total radiation chemical yield of hydroxyl radicals available for further studies amounts to G = 6.1 (the G-value denotes the number of species produced/consumed per 100 eV dissipated energy; G = 1.0 corresponds to 0.1036 μM species per 1 J absorbed energy).

Dimethyl Sulfide. Absorption Characteristics. Figure 1a shows the transient spectrum recorded 120 ns after application of a ca. 5-ns electron pulse to an N_2O-saturated aqueous (H_2O) solution, pH 6.7, containing 2.0 mM dimethyl sulfide (DMS). It is characterized by an absorption maximum at λ_{max} = 340 nm and is formed with a radiation chemical yield of $G\epsilon_{340}$ = 20 130 M^{-1} cm^{-1}. In accordance with earlier studies by Asmus and coworkers[12,13] spectrum a (Figure 1) is assigned to the hydroxyl radical adduct **1a**, formed by simple addition of the pulse radiolytically formed hydroxyl radical to the thioether moiety (reaction 3a). It should be noted at this point that **1a** exists in

$$HO^\bullet + S< \rightarrow \underset{\mathbf{1a}}{HO\text{–}{}^\bullet S<} \qquad (3a)$$

equilibrium with a hydroxyl radical adduct involving two thioether equivalents, >$^\bullet$SSOH. Both species exhibit similar absorption characteristics.[12,13] However, kinetically they are distinguishable through their respective decay processes (see Discussion). Assuming 100% formation of adduct **1a**, its extinction coefficient can be calculated by dividing $G\epsilon_{340}$ by G = 5.9, yielding $\epsilon_{1a,340}$ = 3400 M^{-1} cm^{-1} (the G-value of 5.9 was calculated on the basis of the formula given by Schuler et al. which relates the G-value of solute radicals generated by $^\bullet$OH radicals to the product of the rate constant for the reaction of $HO^\bullet$ with the solute and the solute concentration[20]). Subsequently the 340-nm band disappears with pseudo-first-order kinetics under formation of two new transient absorption bands peaking at λ_{max} = 465 nm and λ_{max} = 285 nm as shown in Figure 1b. The 465-nm band is assigned to the well-characterized[12] three-electron-bonded dimeric radical cation $[(CH_3)_2S.\therefore S(CH_3)_2]^+$ (**2a**) which is formed with $G\epsilon_{465}$ = 32940 M^{-1} cm^{-1}. Taking ϵ_{465} = 6200 M^{-1} cm^{-2} [12] we calculate that the dimeric radical cation is formed with G = 5.3, i.e. to an extent of ca. 90% of initially available hydroxyl radicals. Theoretical considerations have indicated that the dimeric radical cation might have a second absorption band in the UV region

(17) Janata, E.; Schuler, R. H. *J. Phys. Chem.* **1982**, *86*, 2078–2084.
(18) Fricke, H.; Hart, E. J. *J. Chem. Phys.* **1935**, *3*, 60–61.
(19) Von Sonntag, C. *The Chemical Basis of Radiation Biology*; Taylor & Francis: London, 1987.
(20) Schuler, R. H.; Hartzell, A. L.; Behar, B. *J. Phys. Chem.* **1981**, *85*, 192–199.

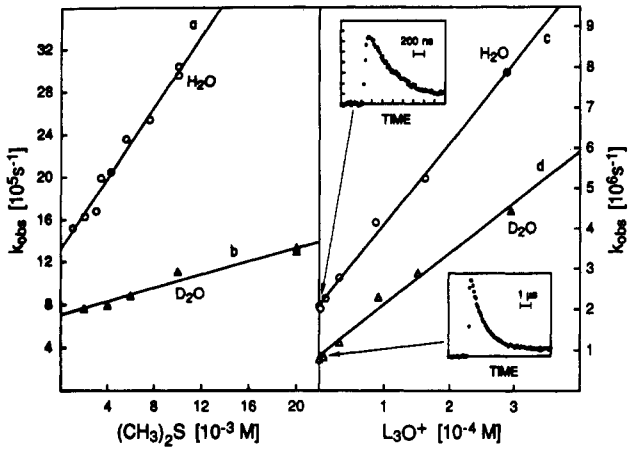

Figure 2. Plots of the observed first-order rate constants of the decay of **1a** (a, c) and **1b** (b, d) as a function of the DMS concentration (at constant pH 6.7/pD 6.9) and L_3O^+ concentration (at constant [DMS] = 2.0 mM), respectively. Insets: Absorption vs time profile of the decay of **1a** at 2.0 mM [DMS] and pH 6.7 (upper), and of **1b** at 2.0 mM [DMS] at pD 6.9 (bottom).

which will in part be responsible for the other absorption band peaking at $\lambda_{max} = 285$.[21] In addition, α-thioether radicals, $CH_3SCH_2^•$, are characterized by a strong absorption band with $\lambda_{max} = 285$ nm[12-15,21,22] ($\epsilon_{285} = 2500\ M^{-1}\ cm^{-1}$ [21,22]). The formation of small amounts of the latter, contributing to the observed band at 285 nm, might account for the residual decay of species **1a** (10%) not leading to the dimeric sulfur radical cation **2a**.

Similar observations were made when experiments were carried out in D_2O (at pD 6.9) instead of H_2O. In the latter system the DO-adduct **1b** is formed according to reaction 3b. Adduct **1b**

$$DO^• + S< \rightarrow \underset{\mathbf{1b}}{DO\text{–}^•S<} \qquad (3b)$$

subsequently decays with pseudo-first-order kinetics into the dimeric radical cation **2a**.

On a longer time scale, i.e. within the millisecond time domain, the dimeric radical cations decay via deprotonation into α-thioether radicals in both solvents, H_2O and D_2O (data not shown here). Processes on this time scale are, however, not under investigation in this paper.

Kinetics. The pseudo-first-order rate constants for the decay of species **1a** (in H_2O) and **1b** (in D_2O) and the parallel buildup of the dimeric radical cation were measured at pH 6.7 and pD 6.9 as a function of the concentration of DMS (varied between 1.0 and 10.0 mM in H_2O and between 2.0 and 20.0 mM in D_2O). Plots of the observed rate constants vs DMS concentration yield straight lines which intercept the *y*-axis at positive values, as shown in Figure 2, parts a and b. The slopes as well as the intercepts show higher values in H_2O than in D_2O. This result indicates the existence of at least two different decay processes of **1a**/**1b**, both of them showing a solvent kinetic isotope effect with $k_{H_2O} > k_{D_2O}$.

The slopes in Figure 2a,b characterize the decay of **1a** and **1b** via reaction with a second thioether molecule according to the general reaction 4, with the respective rate constants being $k_{4,H} = (1.69 \pm 0.2) \times 10^8\ M^{-1}\ s^{-1}$ in H_2O and $k_{4,D} = (0.31 \pm 0.02) \times 10^8\ M^{-1}\ s^{-1}$ in D_2O ($k_H/k_D = 5.4$). The intercepts in Figure

$$\underset{\mathbf{1a/1b}}{} + S< \rightarrow \underset{\mathbf{2a}}{[>S.\therefore S<]^+} + \text{products} \qquad (4)$$

2a,b indicate the operation of an additional decay process, independent of thioether concentration. In a first approach this process might be described as elimination of lyoxide, LO^- (**1a**, L = H; **1b**, L = D), according to eq 5, followed by association of the formed monomeric thioether radical cation with a second nonoxidized thioether according to equilibrium 6 (in H_2O: $k_6 = 3.0 \times 10^9\ M^{-1}\ s^{-1}$, $K_6 = 2.0 \times 10^5\ M^{-1}$ [15]). The rate constants for reaction 5 are derived as $k_{5,H} = (1.32 \pm 0.2) \times 10^6\ s^{-1}$ in H_2O and $k_{5,D} = (0.7 \pm 0.4) \times 10^6\ s^{-1}$ in D_2O ($k_H/k_D = 1.9$).

$$\underset{\mathbf{1a/1b}}{>S^•\text{–}OL} \rightleftharpoons >S^{•+} + {}^-OL \qquad (5)$$

$$>S^{•+} + S< \rightleftharpoons \mathbf{2a} \qquad (6)$$

It had to be ensured that a possible proton-catalyzed dissociation of adducts **1a**/**1b** according to reaction 7 does not play any role in the pH region under investigation. Therefore we investigated the decay of adduct **1a**/**1b** as a function of L_3O^+ concentration over the concentration range of $[H_3O^+] = 1.82 \times 10^{-7}$ M–2.88 $\times 10^{-4}$ M and $[D_3O^+] = 1.15 \times 10^{-6}$ M–2.95 $\times 10^{-4}$ M, using a DMS concentration of 2.0×10^{-3} M. Under these conditions

$$\underset{\mathbf{1a/1b}}{>S^•\text{–}OL} + L_3O^+ \rightarrow >S^{•+} + 2L_2O \qquad (7)$$

the observed rate constant for the decay of species **1a**/**1b** is a composite of three distinct processes and can be expressed via eq I. Plots of the observed first-order rate constants as a function

$$k_{obs} = k_7[L_3O^+] + k_4[DMS] + k_5 \qquad (I)$$

of $[L_3O^+]$ are shown in Figure 2c,d. From the slopes we obtain $k_{7,H} = (2.0 \pm 0.2) \times 10^{10}\ M^{-1}\ s^{-1}$ and $k_{7,D} = (1.26 \pm 0.2) \times 10^{10}\ M^{-1}\ s^{-1}$ ($k_H/k_D = 1.58$). The intercepts correspond to $k_4[DMS] + k_5$. With our measured values for k_4 and [DMS] = 2.0×10^{-3} M we obtain $k_{5,H} = (1.76 \pm 0.2) \times 10^6\ s^{-1}$ and $k_{5,D} = (0.78 \pm 0.05) \times 10^6\ s^{-1}$ ($k_H/k_D = 2.28$). Both values are in good agreement with the intercepts derived from the plots of k_{obs} vs DMS concentration in Figure 2a,b. Taking the rate constants $k_{7,H}$ and $k_{7,D}$ we also easily see that any proton-catalyzed process would be negligible at pH 6.7 and pD 6.9, i.e. under conditions where k_4 and k_5 were measured through variation of the DMS concentration. The mean values for k_5 derived from the two independent determinations amount to $k_{5,H} = (1.54 \pm 0.22) \times 10^6\ s^{-1}$ and $k_{5,D} = (0.74 \pm 0.04) \times 10^6\ s^{-1}$ with $k_H/k_D = 2.09$.

2-(Methylthio)ethanol. Absorption Characteristics. Figure 3a shows the transient spectrum recorded 12 ns after application of a ca. 5-ns electron pulse to an N_2O-saturated aqueous (H_2O) solution, pH 7.4, containing 10^{-1} M 2-MTE. It is composed of two absorption bands peaking at $\lambda_{max} = 285$ nm and $\lambda_{max} = 345$ nm. The 345-nm band disappears in a first-order process within the nanosecond time domain ($\tau_{1/2} = 16$ ns; Figure 3d) paralleled by a further rise of the 285-nm band (Figure 3e) and formation of a small absorption band peaking at $\lambda_{max} = 475$ nm. Figure 3b shows the final spectrum which is fully developed 140 ns after the pulse. In analogy to the results obtained for DMS and published data,[12-16,21,22] the 285-nm band is assigned to an α-thioether radical and the 345-nm band to a hydroxyl radical adduct at the thioether sulfur. The band peaking at 475 nm represents a dimeric three-electron-bonded thioether radical cation from 2-MTE, $[>S.\therefore S<]^+$ (**2c**). The final radiation chemical yields 140 ns after the pulse amount to $G\epsilon_{285} = 14\,000\ M^{-1}\ cm^{-1}$ and $G\epsilon_{475} = 3250\ M^{-1}\ cm^{-1}$. The extinction coefficient for the 285-nm band can be approximated to $\epsilon_{285} \approx 2500\ M^{-1}\ cm^{-1}$ by comparison with values published for α-thioether radicals from DMS[12-14] and methionine.[21,22] The extinction coefficient for the 475-nm band was measured by us as $\epsilon_{475} = 6500\ M^{-1}\ cm^{-1}$ (see below). Division of the radiation chemical yields by the respective extinction coefficients yields *G*-values for both species with $G(\alpha$-

(21) Hiller, K.-O.; Masloch, B.; Göbl, M.; Asmus, K.-D. *J. Am. Chem. Soc.* **1981**, *103*, 2734–2743.
(22) Hiller, K.-O.; Asmus, K.-D. *Int. J. Radiat. Biol.* **1981**, *40*, 597–604.

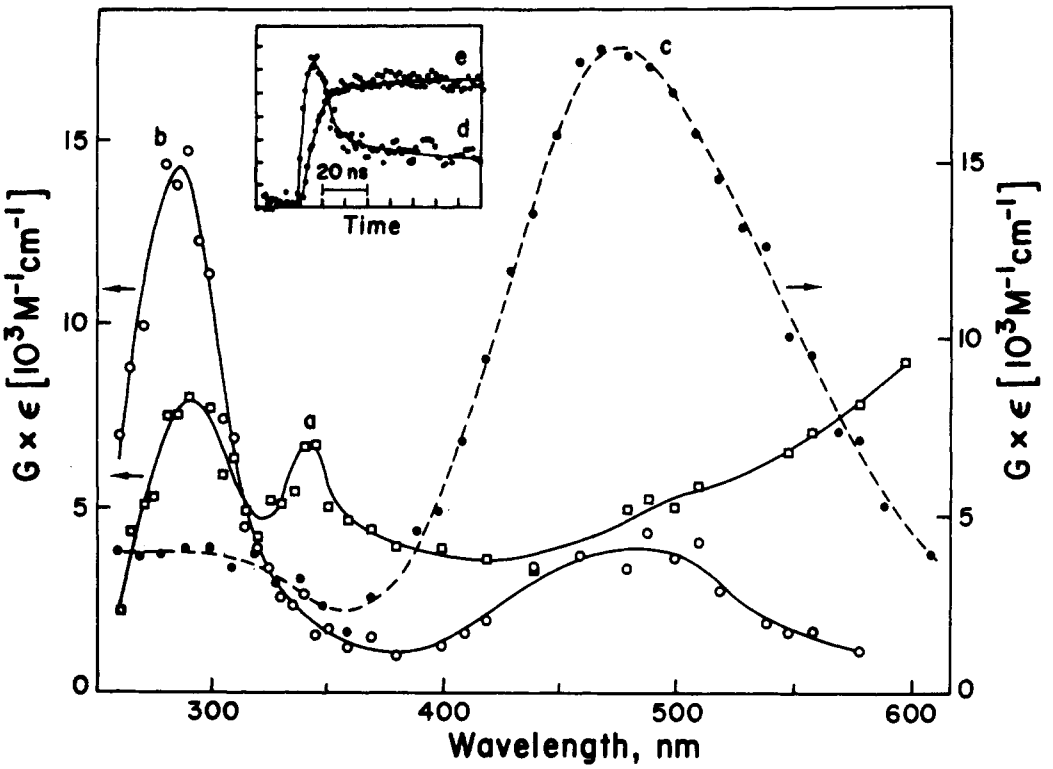

Figure 3. Transient absorption spectra observed (a) 12 ns and (b) 140 ns after pulse irradiation of an N_2O-saturated aqueous solution (H_2O) containing 10^{-1} M 2-MTE at pH 7.4 and (c) 1.4 μs after pulse irradiation of an N_2-saturated solution containing 10^{-2} M 2-MTE at pH 1.0. Inset: Absorption vs time profiles of the decay of **1c** (345 nm) (d) and the formation of α-thioether radicals (285 nm) (e) in N_2O-saturated aqueous (H_2O) solution containing 10^{-1} M 2-MTE at pH 7.4.

thioether radical) = 5.6 and $G([>S.\therefore S<]^+) = 0.5$. Thus 92% of the initially oxidizing hydroxyl radicals react with 2-MTE under conditions of fast formation of α-thioether radicals. The α-thioether radical is rather stable and decays via second-order processes within the millisecond time scale to nonradical products.

Figure 3c shows the spectrum obtained after application of a ca. 5-ns electron pulse to an N_2-saturated aqueous solution (H_2O), pH 1.0, containing 10^{-2} M 2-MTE. These reaction conditions lead to almost exclusive formation of the 475-nm band according to reactions 8 and 9 with $G\epsilon_{475} = 18\,200$ M^{-1} cm^{-1}. Assuming

$$\underset{\mathbf{1c/1d}}{\text{2-MTE(S}^{\bullet}\text{–OL)}} + L_3O^+ \rightarrow \text{2-MTE(S}^{\bullet+}\text{)} + 2L_2O \quad (8)$$

$$\text{2-MTE(S}^{\bullet+}\text{)} + \text{2-MTE(S)} \rightleftharpoons \underset{\mathbf{2c}}{\text{2-MTE(>S.\therefore S<)}^+} \quad (9)$$

that $k_8 \approx k_7$, reaction 8 will be the dominant pathway of adducts **1c/1d** (**1c**, L = H; **1d**, L = D) at pH 1.0 with $\tau_{1/2} \approx 0.35$ ns, compared to all other decay processes occurring with $\tau_{1/2} \geq 16$ ns (see below). The radiation chemical yield of hydroxyl radicals at pH 1.0, available for oxidation of 2-MTE, amounts to $G = 2.8$. Division of $G\epsilon_{475}$ by $G = 2.8$ yields $\epsilon_{475} = 6500$ M^{-1} cm^{-1}, which is comparable to the values of $\epsilon_{465} = 6200$ M^{-1} cm^{-1} and $\epsilon_{505} = 6225$ M^{-1} cm^{-1}, published for the dimeric sulfur radical cations of DMS[12] (**2a**) and of 2,2′-DHE[23] (**2e**), respectively.

Similar observations were made for the reaction of $DO^{\bullet}$ with 2-MTE in D_2O. Under these conditions the alcohol group of $CH_3SCH_2CH_2OH$ undergoes instantaneous H/D exchange with the D_2O solvent. This was confirmed by ^{1}H-NMR experiments showing that the RO–H resonance of 2-MTE measured in $CDCl_3$ ($\delta = 4.13$ ppm) disappeared in D_2O (data not shown). Since all samples were purged for at least 30 min with N_2O prior to pulse irradiation, the H/D exchange, i.e. conversion of $CH_3SCH_2CH_2OH$ into $CH_3SCH_2CH_2OD$, was expected to be completed before the actual experiment.

Kinetics. As for DMS, the formation of a hydroxyl radical adduct constitutes the first step in the oxidation of 2-MTE by hydroxyl radicals (reactions 10a and 10b). However, the decay

$$HO^{\bullet} + \text{2-MTE(S)} \rightarrow \underset{\mathbf{1c}}{\text{2-MTE(S}^{\bullet}\text{–OH)}} \quad (10a)$$

$$DO^{\bullet} + \text{2-MTE(S)} \rightarrow \underset{\mathbf{1d}}{\text{2-MTE(S}^{\bullet}\text{–OD)}} \quad (10b)$$

of the hydroxyl radical adduct is extremely fast and occurs, in part, within the duration of the electron pulse. As a result both the hydroxyl radical adduct and its decay product were observed 12 ns after the pulse. Observation on a shorter time scale was not possible due to limitations in time resolution and pulse width.

The rise of the 285-nm band was measured for 2-MTE in L_2O (L = H, D) as a function of the 2-MTE concentration (>2×10^{-2} M) (bottom inset in Figure 4). In addition, at high concentrations of 2-MTE (>8.0×10^{-2} M), the parallel decay of the 345-nm band was measured. The first-order rate constants derived at both wavelengths were identical. Figure 4, parts a and b show plots of the observed first-order rate constants as a function of 2-MTE concentration. Straight lines were obtained for 2-MTE concentrations larger than 2.0×10^{-2} M, which intercept the y-axis at positive values. Again, at least two distinct processes lead to the decomposition of the hydroxyl radical adduct, one being dependent on and one being independent of 2-MTE concentration as outlined in reactions 11 and 12. As derived

$$\mathbf{1c/1d} + \text{2-MTE(S)} \rightarrow \underset{\mathbf{2c}}{\text{2-MTE(>S.\therefore S<)}^+} + \text{products} \quad (11)$$

$$\mathbf{1c/1d} \rightarrow \text{products} \quad (12)$$

from the slopes of the straight lines, the formation of the dimeric

(23) Mohan, H.; Mittal, J. P. *Radiat. Phys. Chem.* **1991**, *38*, 45–50.

radical cation occurs via interaction with a second nonoxidized thioether molecule, with the bimolecular rate constants being $k_{11,H} = (7.7 \pm 0.3) \times 10^7$ M^{-1} s^{-1} and $k_{11,D} = (5.0 \pm 1.0) \times 10^7$ M^{-1} s^{-1}. Although not as large as for the thioether concentration-dependent process of DMS, still a measurable kinetic isotope effect with $k_H/k_D = 1.54$ is observed for the corresponding reaction 11 of 2-MTE.

In contrast to the DMS system, the intercepts in Figure 4, parts a and b, corresponding to the reaction 12 of 2-MTE, show a small inverse kinetic isotope effect with $k_{12,H} = (6.32 \pm 0.7) \times 10^7$ s^{-1} and $k_{12,D} = (6.99 \pm 0.7) \times 10^7$ s^{-1} ($k_H/k_D = 0.9$).

Since the decay of adducts **1c**/**1d** was so fast, we had to ensure that their formation, i.e. reactions 10a and 10b, were not rate-limiting for the derivation of k_{11} and k_{12}. For measuring these rate constants the buildup of the 285-ns band was monitored under experimental conditions where reactions 10a and 10b were, in fact, rate-determining, i.e. at low concentrations of 2-MTE (5.0×10^{-5}–5.0×10^{-4} M). Respective plots of the observed pseudo-first-order rate constants for the formation of the 285-nm band vs 2-MTE concentration yield straight lines. From the slopes we derive $k_{10a} = (7.90 \pm 0.20) \times 10^9$ M^{-1} s^{-1} and $k_{10b} = (8.02 \pm 0.64) \times 10^9$ M^{-1} s^{-1}. As expected we do not observe a kinetic solvent isotope effect for the formation of **1c** and **1d**. Using the obtained rate constants we also see that under the conditions employed for deriving k_{11} and k_{12} ([2-MTE] > 2.0×10^{-2} M) reactions 10a and 10b are not rate-limiting.

2,2′-Dihydroxydiethyl Sulfide. Kinetics. As for 2-MTE, the pulse irradiation of N_2O-saturated solutions of 10^{-1} M 2,2′-DHE solutions in H_2O (pH 7.2) and D_2O (pD 7.4) leads to the formation of both the transient 345-nm and the 285-nm band ca. 12 ns after the pulse. The appearance of the 345-nm band is indicative of formation of the hydroxyl radical adducts **1e** and **1f** according to reactions 13a and 13b. The formation of **1e** and **1f** was measured to occur with $k_{13a} = (8.14 \pm 0.4) \times 10^9$ M^{-1} s^{-1} and $k_{13b} = (8.28 \pm 0.4) \times 10^9$ M^{-1} s^{-1}. Subsequently the 345-nm

$$HO^{\bullet} + \text{2,2′-DHE(S)} \rightarrow \underset{\textbf{1e}}{\text{2,2′-DHE(S}^{\bullet}\text{–OH)}} \quad (13a)$$

$$DO^{\bullet} + \text{2,2′-DHE(S)} \rightarrow \underset{\textbf{1f}}{\text{2,2′-DHE(S}^{\bullet}\text{–OD)}} \quad (13b)$$

band converts into the 285-nm band within the nanosecond time domain (top inset in Figure 4). The lifetimes of the hydroxyl radical adducts **1e** and **1f** depend on the concentration of 2,2′-DHE. Plots of the observed pseudo-first-order rate constants of **1e**/**1f** vs the concentration of 2,2′-DHE yield similar plots as for 2-MTE, indicating the occurrence of reactions 14 and 15 (Figure 4c,d). No kinetic isotope effect is observed for the thioether and

$$\textbf{1e/1f} + \text{2,2′-DHE} \rightarrow \underset{\textbf{2e}}{\text{2,2′-DHE(>S}\therefore\text{S<)}^{+}} + \text{products} \quad (14)$$

$$\textbf{1e/1f} \rightarrow \text{products} \quad (15)$$

proton concentration-independent decay process with $k_{15,H} = (1.17 \pm 0.2) \times 10^8$ s^{-1} and $k_{15,D} = (1.13 \pm 0.2) \times 10^8$ s^{-1}. Also the observed kinetic isotope effect for the thioether concentration-dependent decay is relatively small with $k_{14,H} = (1.65 \pm 0.2) \times 10^8$ M^{-1} s^{-1} and $k_{14,D} = (1.38 \pm 0.2) \times 10^8$ M^{-1} s^{-1} ($k_H/k_D = 1.19$). Table I summarizes all rate constants obtained for the oxidation of DMS, 2-MTE, and 2,2′-DHE, including their respective kinetic isotope effects.

A few remarkable differences between the DMS system and 2-MTE and 2,2′-DHE are already noted. First, the decay of the hydroxyl radical adducts **1c**, **1d**, **1e**, and **1f**, independent of thioether and proton concentration, occurs more than 1 order of magnitude faster than the decay of the same adducts at DMS.

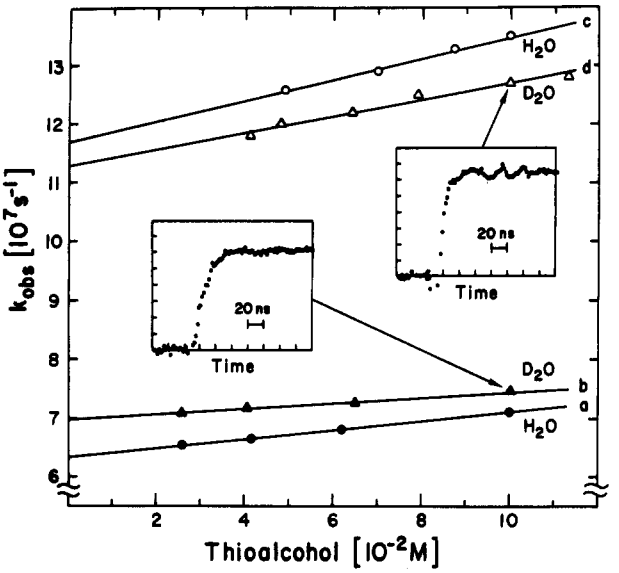

Figure 4. Plots of observed first-order rate constants of the formation of an α-thioether radical (285 nm) as a function of 2-MTE concentration in H_2O (a) and D_2O (b) at constant pH 7.4 and pD 7.4, respectively, as a function of 2,2′-DHE concentration in H_2O (c) and D_2O (d) at constant pH 7.2 and pD 7.4, respectively. Insets: Absorption vs time profiles of the formation of α-thioether radicals in D_2O containing 10^{-1} M 2-MTE (left) and 10^{-1} M 2,2′-DHE (right).

Table I. Rate Constants and Kinetic Isotope Effects for the Hydroxyl Radical Induced Oxidation of DMS, 2-MTE, and 2,2′-DHE

	Formation of Hydroxyl Radical Adducts	
DMS	$k_{3,H} = (1.90 \pm 0.5) \times 10^{10}$ M^{-1} s^{-1} [12]	
2-MTE	$k_{10a} = (7.90 \pm 0.2) \times 10^9$ M^{-1} s^{-1}	
	$k_{10b} = (8.02 \pm 0.64) \times 10^9$ M^{-1} s^{-1}	$k_H/k_D = 0.99$
2,2′-DHE	$k_{13a} = (8.14 \pm 0.4) \times 10^9$ M^{-1} s^{-1}	
	$k_{13b} = (8.28 \pm 0.4) \times 10^9$ M^{-1} s^{-1}	$k_H/k_D = 0.98$
	Thioether Concentration-Independent Decomposition of the Hydroxyl Radical Adduct	
DMS	$k_{5,H} = (1.54 \pm 0.22) \times 10^6$ s^{-1}	
	$k_{5,D} = (0.74 \pm 0.04) \times 10^6$ s^{-1}	$k_H/k_D = 2.09$
2-MTE	$k_{12,H} = (6.32 \pm 0.7) \times 10^7$ s^{-1}	
	$k_{12,D} = (6.99 \pm 0.7) \times 10^7$ s^{-1}	$k_H/k_D = 0.90$
2,2′-DHE	$k_{15,H} = (1.17 \pm 0.2) \times 10^8$ s^{-1}	
	$k_{15,D} = (1.13 \pm 0.2) \times 10^8$ s^{-1}	$k_H/k_D = 1.04$
	Thioether Concentration-Dependent Decomposition of the Hydroxyl Radical Adduct	
DMS	$k_{4,H} = (1.69 \pm 0.2) \times 10^8$ M^{-1} s^{-1}	
	$k_{4,D} = (0.31 \pm 0.02) \times 10^8$ M^{-1} s^{-1}	$k_H/k_D = 5.40$
2-MTE	$k_{11,H} = (7.7 \pm 0.3) \times 10^7$ M^{-1} s^{-1}	
	$k_{11,D} = (5.0 \pm 1.0) \times 10^7$ M^{-1} s^{-1}	$k_H/k_D = 1.54$
2,2′-DHE	$k_{14,H} = (1.65 \pm 0.2) \times 10^8$ M^{-1} s^{-1}	
	$k_{14,D} = (1.38 \pm 0.2) \times 10^8$ M^{-1} s^{-1}	$k_H/k_D = 1.19$

Second, the unimolecular decay of **1c**–**f** shows almost no kinetic solvent isotope effect and, finally, does not lead to the formation of sulfur–sulfur-bonded dimeric radical cations.

3,3′-Dihydroxydipropyl Sulfide. Absorption Characteristics and Kinetics. Pulse irradiation of an N_2O-saturated aqueous solution (H_2O), pH 7.0, containing 10^{-2} M 3,3′-dihydroxydipropyl sulfide (3,3′-DHP) leads to the formation of an absorption band with an apparent $\lambda_{max} = 370$ nm ca. 34 ns after the pulse (Figure 5a), which subsequently converts with first-order kinetics into a band with $\lambda_{max} = 410$ nm ($\tau_{1/2} = 40$ ns) (Figure 5b). The 410-nm band disappears in a first-order process with $\tau_{1/2} = 6.3$ μs, paralleled by the buildup of an absorption band with $\lambda_{max} = 490$ nm (Figure 5c). By comparison with spectra published for a series of thioethers containing additional oxygen functional groups

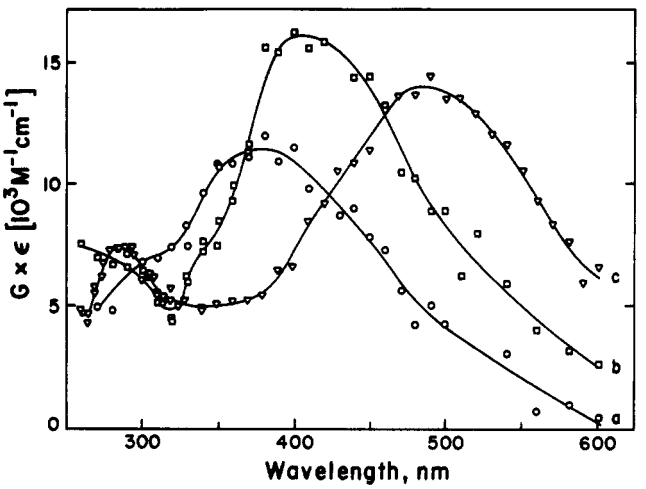

Figure 5. Transient absorption spectra observed (a) 34 ns, (b) 262 ns, and (c) 15 μs after pulse irradiation of an N_2O-saturated aqueous solution (H_2O) containing 10^{-2} M 3,3′-DHP at pH 7.0.

(including 3,3′-DHP),[24] the latter spectrum is attributed to a three-electron-bonded dimeric thioether radical cation of 3,3′-DHP. The 410-nm band is assigned to the three-electron sulfur–oxygen bonded structure **3**.[24] The 370-nm band observed 34 ns after the pulse is believed to be a composite of both the arising 410-nm band and the disappearing spectrum of the initially formed hydroxyl radical adduct at 3,3′-DHP. The latter will most probably show an absorption maximum between λ = 330 and 345 nm. Due to the rapid conversion of the hydroxyl radical adduct into **3**, both species cannot be resolved experimentally at

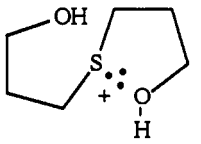

3

the employed 3,3′-DHP concentration. The use of higher concentrations is limited by the solubility of 3,3′-DHP. Species **3** is formed in the reaction sequence 16 and 17.

$$HO^{\bullet} + 3,3'\text{-DHP} \rightarrow 3,3'\text{-DHP}(S^{\bullet}\text{–OH}) \qquad (16)$$

$$3,3'\text{-DHP}(S^{\bullet}\text{–OH}) \rightarrow \mathbf{3} + HO^{-} \qquad (17)$$

Unlike the reaction sequences for 2-MTE and 2,2′-DHE the hydroxyl radical adduct at 3,3′-DHP does not decay into α-thioether radicals within the nanosecond time domain but, instead, under formation of species **3**.

Formaldehyde Yields. The γ-radiolysis of N_2O-saturated aqueous solutions at pH 1.0 and 6.5 containing 2-MTE, 2,2′-DHE, or 3,3′-DHP at 10^{-2} M concentration, respectively, leads to the yields of formaldehyde shown in Table II. The *G*-values were calculated from the straight lines derived by plotting the measured formaldehyde concentrations vs the applied radiation dose for five different doses. High formaldehyde yields are derived for experiments with 2-MTE ($G = 3.2$) and 2,2′-DHE ($G = 2.64$) at pH 6.5, accounting for ca. 52% and 43% of initially available hydroxyl radicals ($G = 6.1$). On the other hand, very low yields are obtained in experiments carried out at pH 1.0, and under all conditions for 3,3′-DHP.

(24) (a) Mahling, S.; Asmus, K.-D.; Glass, R. S.; Hojjatie, M.; Wilson, G. S. *J. Org. Chem.* **1987**, *52*, 3717–3724. (b) Mohan, H.; Mittal, J. P. *J. Chem. Soc., Perkin Trans. 2* **1992**, 207–212. (c) Mohan, H. *J. Chem. Soc., Perkin Trans. 2* **1990**, 1821–1824.

Scheme I

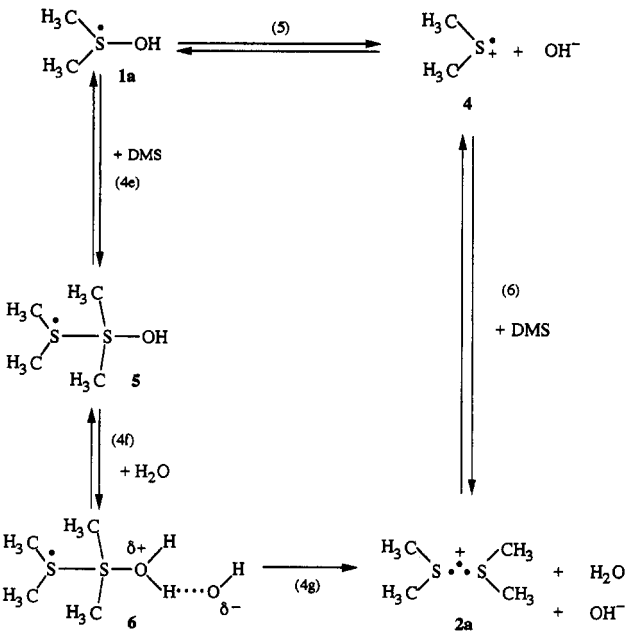

Discussion

Decomposition of the Hydroxyl Radical Adduct of DMS. Two major factors might contribute to a solvent kinetic isotope effect:[25,26] (i) secondary effects from protons which can exchange with protons from the solvent but are not directly involved in a rate-determining proton-transfer step in a chemical process and (ii) primary contributions from protons which directly undergo proton transfer in a rate-determining step. The product of both yields the overall solvent kinetic isotope effect:[25,26]

$$(k_H/k_D)_{exp} = (k_H/k_D)_{prim}(k_H/k_D)_{sec} \qquad (II)$$

The secondary contributions can generally be estimated by defining the fractionation factors, φ, for the respective reactants and products or a transition state.[25,26] According to Schowen[25] an isotopic fractionation factor for any particular site in a molecule is defined as the ratio of its preference for deuterium over protium relative to the similar preference of a single site in a solvent molecule. The fractionation factors for the most common functional groups are tabulated.[26]

For convenience the following discussion will be based on reactions in H_2O using the notations for the respective intermediates in H_2O. The hydroxyl radical induced oxidation of DMS proceeds via formation of the hydroxyl radical adduct **1a**, which almost exclusively converts into the three-electron-bonded dimeric radical cation **2a**. Two distinct processes contributing to the decay of **1a** have been identified in agreement with earlier observations by Asmus et al. in H_2O.[12–14] On the basis of the relatively large kinetic isotope effects observed for the reactions 4 and 5, we can now formulate the underlying mechanisms in more detail as outlined in Scheme I.

According to equilibrium 5 the hydroxyl radical adduct **1a** decays in a unimolecular process into the monomeric radical cation **4**, which subsequently associates with a second nonoxidized thioether in equilibrium 6. The observed solvent kinetic isotope effect for this reaction sequence is $(k_H/k_D)_{exp} = 2.09$. An estimate for a contribution of secondary effects can be obtained through division of the product of the fractionation factors of the reactants by the product of the fractionation factors of the reaction products, $(k_H/k_D)_{sec} = \phi(\mathbf{1a})/\phi(LO^-)\phi(\mathbf{4})$.[25,26] In analogy to organic alcohols we assume that $\phi(\mathbf{1a}) = 1.0$.[26] Species **4** has no readily

(25) Schowen, R. L. *Prog. Phys. Org. Chem.* **1972**, *9*, 275–332.
(26) Alvarez, F. J.; Schowen, R. L. In *Isotopes in Organic Chemistry*; Buncel, E., Lee, G. C., Eds.; Elsevier: NY, 1987; pp 1–60.

exchangeable protons, and therefore, we take $\phi(4) = 1.0$. With $\phi(LO^-) = 0.5$[26] we derive $(k_H/k_D)_{sec} = 2.0$. This value is in fairly good agreement with our experimentally observed kinetic isotope effect, i.e. $(k_H/k_D)_{sec} \approx (k_H/k_D)_{exp}$. The contribution of any primary isotope effect might be negligible, i.e. $(k_H/k_D)_{prim} \approx 1.0$. Therefore no proton transfer, e.g. from water, seems to be involved in the rate-determining step for the decay of adduct **1a**. Thus, reactions 5 and 6 likely represent the true decay mechanism of **1a**. It should be noted that the agreement between the observed kinetic solvent isotope effect and the prediction on the basis of the fractionation factors suggests that the transition state for reaction 5 might closely resemble the products, [**4**] + OH^-.

The thioether concentration-dependent decay of **1a** shows a relative high kinetic isotope effect of $k_H/k_D = 5.4$. This cannot be explained by simply involving a displacement process as in equation 4a. For the latter we would expect a kinetic isotope effect on the order of $k_H/k_D = 2.0$ in accord with the considerations for reaction 5. The high experimentally observed kinetic isotope

$$>S + >S^{\bullet}\text{–}OH \rightarrow [>S.\therefore S<]^+ + OH^- \qquad (4a)$$

effect rather suggests the involvement of a rate-determining proton-transfer step in the overall decay of **1a**.

High kinetic isotope effects, rationalized by rate-limiting proton-transfer steps, were measured for the reactions of methoxyamine with benzaldehyde[27] $[(k_H/k_D)_{max} \approx 3.0]$ and phenyl acetate[28] $[(k_H/k_D)_{max} \approx 4.0]$ catalyzed by weak acids. Lower kinetic isotope effects, i.e. $(k_H/k_D) \approx 1.4$–1.5, were obtained for catalysis by stronger acids.[27,28] These reactions were proposed to proceed in a three-step mechanism involving preassociation of both reactants and acid, proton transfer, and dissociation as outlined in the eq 4b–d (N = nucleophile, E = electrophile, HA = acid). In such a sequence the proton-transfer step (4c) would

$$N + E + HA \underset{(4a)}{\rightleftharpoons} NE{\cdot}HA \underset{(4c)}{\rightleftharpoons} NEH{\cdot}A \underset{(4d)}{\rightarrow} \text{products}$$

be rate-limiting whenever the pK_a difference of the two bases between which the proton is shifted, i.e. the A^- and the NE moiety, was $\Delta pK_a \approx 0$. Formation of the encounter complex (reaction 4b) would be rate-limiting for $\Delta pK_a \ll 0$ and dissociation (reaction 4d) rate-determining for $\Delta pK_a \gg 0$. Furthermore, the proton transfer by weaker acids should be preceded by considerable solvation changes around the forming anion A^-.

A somewhat comparable pathway might account for the high solvent kinetic isotope effect observed for the thioether concentration-dependent decay of **1a** as delineated in Scheme I. Adduct **1a** reacts with a second thioether molecule in a fast equilibrium (4e) to form species **5**, which might also be preassociated with water since water is the actual solvent. Kinetic evidence for the formation of a "**5**-like" species from tetrahydrothiophene was presented earlier by Asmus and co-workers.[13] Intermediate **5** undergoes proton transfer (reaction 4f) via transition structure **6**, which subsequently decays into the products water, OH^-, and **2a** (reaction 4g).

The hydroxyl radical adduct **5** should be considerably polarized with a higher density of negative charge on the more electronegative oxygen atom. It might be described by the structure $>S\text{–}S^{(\delta+)}\text{–}O^{(\delta-)}H$. A comparable charge separation has been postulated, for example, for adducts of peroxyl radicals[29] and singlet oxygen[30] with thioethers. Therefore the pK_a values of the two bases involved in the proton transfer, namely, $>S\text{–}S^{(\delta+)}\text{–}O^{(\delta-)}H$ and OH^-, might not be very different from each other. As a result we will approximately meet conditions of $\Delta pK_a \approx 0$ which would render the proton transfer rate-determining according to the considerations above. Reaction 4g simply represents a shift of positive charge from the oxygen to the sulfur and should be faster than the proton transfer from water. In addition, a second thioether molecule is already part of the structure which would favor the formation of the highly stabilized dimeric adduct **2a**.

The proton transfer from water, however, not only should be associated with a primary kinetic isotope effect but also should show secondary contributions due to the separation of charge in the transition structure **6**. These can be estimated by involving the fractionation factors for the reactants and the transition state.[25,26] Equation III yields the theoretically expected secondary kinetic isotope effect considering only nontransferred protons for conditions in which a proton is transferred from water to the hydroxyl group of **5** (δ corresponds to the position of the transition state on the reaction coordinate). If the developing positive charge

$$(k_H/k_D)_{sec} = [\phi(\mathbf{5})\ \phi(L_2O)]/[\phi^{\delta}(LO^-)\ \phi^{\delta}(\mathbf{6})] \qquad (III)$$

in **6** resides exclusively on the hydroxyl oxygen we should employ a fractionation factor $\phi(>S\text{–}SOH^+) \approx 0.69$ in analogy to protonated alcohols.[26] Taking[26] $\phi(L_2O) = 1.0$, $\phi(\mathbf{5}) = 1.0$ (in analogy to alcohols), and $\phi(LO^-) = 0.5$, a theoretical maximum of $(k_H/k_D)_{sec,max} = 2.9$ can be calculated for $\delta = 1.0$ (case 1). However, if the overall positive charge resides more on the sulfur than on the oxygen atom, the fractionation factor $\phi(>S\text{–}^{(+)}SOH)$ will probably be closer to 1.0 (comparable to the fractionation factor for alcohol functionalities, ROH).[26] Under these conditions the maximum expected secondary isotope effect for $\delta = 1.0$ will be $(k_H/k_D)_{sec,max} \approx 2.0$ (case 2).

Inserting these limiting numbers into eq II we see that the minimum values for the primary contributions to the overall isotope effect will be $(k_H/k_D)_{prim,min} = 1.86$ (case 1) and $(k_H/k_D)_{prim,min} = 2.7$ (case 2).

The H_3O^+-catalyzed decay of **1a** shows a much lower kinetic isotope effect of $k_H/k_D = 1.58$ (reactions 4e, 7a, and 7b). This result is in accord with kinetic isotope effects of ca. 1.4–1.5 which were observed for carboxylic acid catalysis of the methoxyaminolysis of phenyl acetate under conditions of $\Delta pK_a \ll 0$.[27,28] We can reasonably assume that the pK_a of H_2O should be lower than the pK_a of $>S\text{–}S^{(\delta+)}\text{–}O^{(\delta-)}H$, and therefore $\Delta pK_a < 0$, which would make the actual proton transfer in reaction 7a less rate-determining.

$$\underset{\mathbf{1a}}{>S^{\bullet}\text{–}OH} + S< \rightleftharpoons \underset{\mathbf{5}}{>^{\bullet}S\text{–}S\text{–}OH} \qquad (4e)$$

$$\mathbf{5} + H_3O^+ \rightleftharpoons >^{\bullet}S\text{–}S\text{–}OH_2^+ + H_2O \qquad (7a)$$

$$>^{\bullet}S\text{–}S\text{–}OH_2^+ \rightarrow [>S.\therefore S<]^+(OH_2) \qquad (7b)$$

At present we would not like to attempt a more detailed absolute determination and rationalization of both primary and secondary contributions to the observed kinetic isotope effects since too many variables are unknown. However, with some certainty we can define the two mechanisms leading to the decay of the hydroxyl radical adduct **1a** of DMS. A pure dissociation mechanism operates in the thioether concentration-independent pathway, whereas the thioether concentration-dependent reaction involves water/proton catalysis. The characteristic isotope effects will be used in the following as a basis for the investigation of the reaction mechanisms of hydroxyl radical adducts of (alkylthio)ethanol derivatives.

The Thioether Concentration-Dependent Decomposition of Hydroxyl Radical Adducts of 2-MTE and 2,2′-DHE. The oxidation of (alkylthio)ethanol derivatives leads to the formation of dimeric sulfur radical cations *only* in the thioether concentration-dependent decay of hydroxyl radical adducts **1c**/**1e** (**c** from 2-MTE; **e**, from 2,2′-DHE), whereas the thioether con-

(27) Bergman, N.-A.; Chiang, Y.; Kresge, A. J. *J. Am. Chem. Soc.* **1978**, *100*, 5954–5956.
(28) Cox, M. M.; Jencks, W. P. *J. Am. Chem. Soc.* **1981**, *103*, 572–580.
(29) Schöneich, Ch.; Aced, A.; Asmus, K.-D. *J. Am. Chem. Soc.* **1991**, *113*, 375–376.
(30) Jensen, F.; Foote, C. S. *J. Am. Chem. Soc.* **1988**, *110*, 2368–2375.

Scheme II

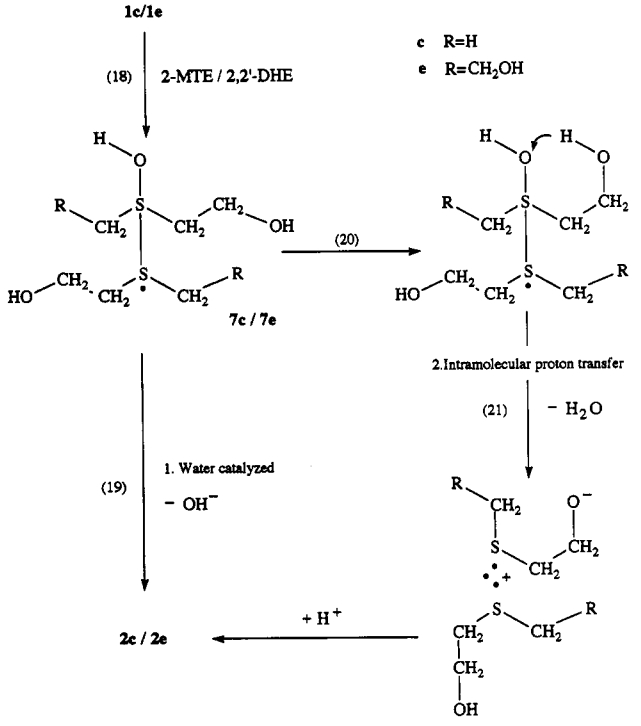

centration-independent pathway leads to α-thioether radicals. Let us first examine the thioether concentration-dependent pathway. The kinetic solvent isotope effect for reaction 11 of 2-MTE amounts to $k_H/k_D = 1.54$, whereas the one for reaction 14 of 2,2'-DHE is even lower, with $k_H/k_D = 1.19$. As for DMS we propose the fast addition of a second nonoxidized thioether molecule to **1c** or **1e** leading to the intermediates **7c/7e**, preceding the formation of **2c/2e** (reaction 18, Scheme II). Subsequently two possible pathways may lead to the elimination of water. A water-catalyzed mechanism according to reaction 19 will occur as discussed for DMS. In addition a proton might be transferred intramolecularly from the adjacent alcohol hydroxyl group (reaction 21). The latter proton transfer will benefit from a particularly favorable six-membered transition structure which might form via conformational rearrangement of structure **7c/7e** according to reaction 20. Proton-transfer reactions within spatially close arrangements have been shown to proceed extremely fast.[31] For example, proton transfer from dodecylammonium propionate to excited pyrene-1-carboxylate within reversed micelles occurred with a rate constant of 2.0×10^{12} M^{-1} s^{-1}.[31] The actual proton transfer within the six-membered structure is therefore not expected to be rate-limiting for the decay of **1c/1e** via reactions 18, 20, and 21, and therefore we do not expect a pronounced kinetic isotope effect. It will be discussed below that it might rather be the formation of the cyclic structure itself (reaction 20) which is rate-limiting. On the other hand, the water-catalyzed formation of **2c** and **2e** (reaction 19) should, in principle, show an isotope effect similar to the same process for DMS, i.e. $k_H/k_D = 5.4$. The overall observed kinetic isotope effect will, therefore, depend on the extent to which reactions 19 or 20 and 21 contribute to the formation of **2c/2e**. The more reactions 20 and 21 dominate the process, the lower the kinetic isotope effect expected. A comparison of $k_H/k_D = 1.5$ for 2-MTE with $k_H/k_D = 5.4$ for DMS shows that the overall contribution of reaction 19 for 2-MTE is already relatively small. 2,2'-DHE provides two hydroxyethyl substituents and, therefore, an even higher probability for the occurrence of reactions 20 and 21. In accord we observe an even lower kinetic isotope effect of $k_H/k_D = 1.19$ for the thioether concentration-dependent decay of the hydroxyl radical adduct of 2,2'-DHE. (In the following it will be shown that a hydrogen transfer via a cyclic six-membered transition state leads to radical fragmentation of 2-MTE and 2,2'-DHE monomers in a unimolecular mechanism. If such a hydrogen transfer would occur in adducts **7c/7e** instead of proton transfer via reactions 20 and 21, we should not see the thioether dependent formation of sulfur–sulfur-bonded dimeric radical cations. Thus the occurrence of a hydrogen-transfer mechanism in adducts **7c/7e** might be ruled out.)

The Thioether Concentration-Independent Decomposition of Hydroxyl Radical Adducts of 2-MTE and 2,2'-DHE. The thioether concentration-independent decay of **1c/1e** leads to the formation of α-thioether radicals. These reactions show a small inverse kinetic isotope effect for 2-MTE, show no kinetic isotope effect for 2,2'-DHE, and occur very fast with $k_{12,H} = (6.32 \pm 0.7) \times 10^7$ s^{-1} and $k_{15,H} = (1.15 \pm 0.2) \times 10^8$ s^{-1}. They are faster than deprotonation reactions from monomeric thioether radical cations, a possible alternative for α-thioether radical formation according to the general reaction 22.[15] These occur with rate constants on the order of $k_{21} = 1.3 \times 10^6$ s^{-1} (for DMS),[15] i.e. more than 1 order of magnitude slower. Thus deprotonation processes as in

$$RCH_2S^{\bullet+}\text{–}CH_2R \rightarrow H^+ + RC^{\bullet}HSCH_2R \qquad (22)$$

reaction 22 can be ruled out for the fast formation of α-thioether radicals of 2-MTE and 2,2'-DHE. A mechanistically attractive alternative for the fast formation of α-thioether radicals is a rapid intramolecular hydrogen transfer from the adjacent alcohol hydroxyl groups via the six-membered transition state **8c/8e** depicted in Scheme III. Hydrogen transfer leads to the formation of highly reactive alkoxyl radicals **9c/9e** via elimination of water, according to reaction 24. Intermediate **9c/9e** has two possibilities for the subsequent formation of α-thioether radicals. First, an intramolecular hydrogen transfer from the δ-carbon atom might proceed, again via a six-membered transition state (reaction 25), analogous to the well-known Barton reaction.[32] As a second alternative, α,β-cleavage (reaction 26) might compete, leading to α-thioether radicals and formaldehyde. This occurs in particular because it is established that α,β-cleavage of alkoxyl radicals is especially fast in polar solvents.[33] As indicated in Table II, high yields of formaldehyde were obtained in the γ-radiolysis of 2-MTE and 2,2'-DHE at pH 6.5, indicating the existence of this second pathway. From the formaldehyde yields we conclude that both pathways occur with ca. 50% probability.

It is remarkable that the overall decay of **1c/1e**, as well as the formation of α-thioether radicals, does not show a kinetic isotope effect. This would exclude reaction 24 as the rate-limiting step. If instead reaction 23, i.e. the formation of the transition structure **8c/8e**, would be rate-limiting, we might estimate the activation energy of the overall process from the rotational barriers of **1c/1e**. These are not known. However, Fausto et al.[34] calculated the rotational barriers of $CH_3SCH_2CH_3$ in the gas phase. If the sum of the rotational barriers of methyl ethyl sulfide is taken as a rough approximation for the rotational barriers of the HO–$^{\bullet}SCH_2CH_2OH$ moiety in **1c/1e** and represent the energy of activation for the formation of **8c/8e**, then we obtain $k_{23} = (5\text{–}10) \times 10^7$ s^{-1} using $k = A \exp(E_a/RT)$ with $A = 10^{13}$ s^{-1} and $T = 298$ K. This value does not deviate much from the rate constants for the decay of **1c/1e** measured in our system and might indicate the possibility that conformational rearrangement of **1c/1e** (reaction 23) could be indeed rate-limiting.

The differences between the observed solvent kinetic isotope effects for the unimolecular decomposition pathways of the

(31) Escabi-Perez, J. R.; Fendler, J. H. *J. Am. Chem. Soc.* **1978**, *100*, 2234–2236.

(32) For an overview see: Carruthers, W. *Some Modern Methods of Organic Synthesis*; Cambridge University Press: NY, 1986; pp 269–279.

(33) Avila, D. V.; Brown, C. E.; Ingold, K. U.; Lusztyk, J. *J. Am. Chem. Soc.* **1993**, *115*, 466–470.

(34) Fausto, R.; Teixeira-Dias, J. J. C.; Carey, P. R. *J. Mol. Struct.* **1987**, *159*, 137–152.

Scheme III

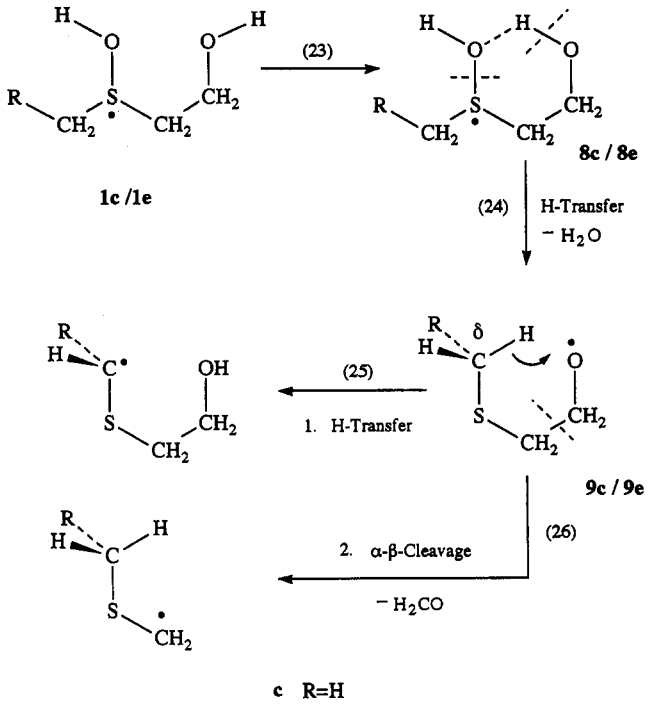

Table II. Yields of Formaldehyde in *G*-Values as Derived from HPLC Analysis of γ-Irradiated N_2O-Saturated Solutions at Different pH's Containing 10^{-2} M Thioether[a]

	G(H2C=O)	
	pH 1.0	pH 6.5
2-MTE	<0.20 ± 0.1	3.20 ● 0.3
2,2′-DHE	<0.10 ● 0.1	2.64 ± 0.3
3,3′-DHP	<0.20 ± 0.1	<0.20 ± 0.1

[a] Conditions: see text.

hydroxyl radical adducts of DMS and the (alkylthio)ethanol derivatives is, therefore, rationalized by the occurrence of entirely different decay mechanisms. In the case of DMS a dissociation of the hydroxyl radical adduct into HO^- and $>S^{\bullet+}$ takes place. In contrast, the (alkylthio)ethanol derivatives eliminate H_2O (instead of HO^-), formed via a fast intramolecular hydrogen transfer.

Two other alternative mechanisms which might lead to the formation of formaldehyde should be discussed briefly. First, a proton rather than a hydrogen atom might be transferred in the six-membered structure **8c/8e** leading to intermediate **10c/10e** as shown in Scheme IV (reaction 27). The alkoxide moiety might displace the water molecule by intramolecular nucleophilic attack at the sulfur, leading to the four-membered oxathietane intermediate **11c/11e** (reaction 28), which subsequently might suffer fragmentation into formaldehyde and α-thioether radicals (reaction 29) in analogy to the cleavage of dioxetane systems.[35] Two arguments speak against the contribution of such a mechanism. On one hand, formation of stable four-membered-ring structures of three-electron-bonded S∴X intermediates with X = N or O have so far never been observed.[22,36] We would expect structure **11c/11e** to undergo fast ring opening (reaction 30) in competition with the fragmentation reaction 29. Species **12c/12e** should rapidly protonate at the alkoxide oxygen and associate with a second thioether molecule to yield dimeric thioether radical cations **2c/2e**, especially at the high thioether concentrations used. The experimentally observed yields of **2c/2e** were, however, rather low (≤8%). If, on the other hand, formation of the cyclic

(35) Adam, W.; Baader, W. J. *J. Am. Chem. Soc.* **1985**, *107*, 410–416.
(36) Asmus, K.-D.; Göbl, M.; Hiller, K.-O.; Mahling, S.; Mönig, J. *J. Chem. Soc., Perkin Trans. 2* **1985**, 641–646.

Scheme IV

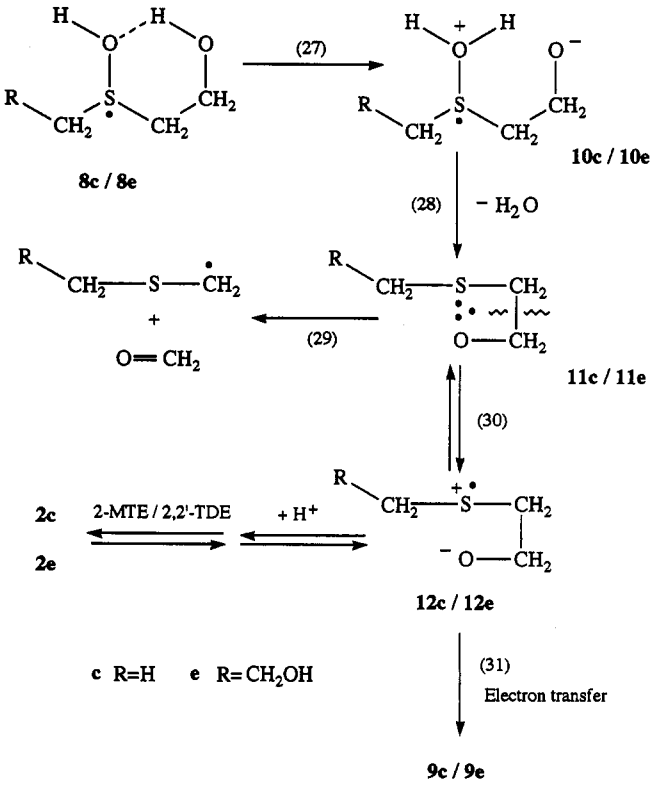

intermediate **11c/11e** were a highly favorable process, we would expect species **2c/2e** to dissociate into monomeric radical cations, which subsequently should undergo ring closure to form **11c/11e**. The latter would fragment into formaldehyde and α-thioether radicals. Therefore experiments were performed at pH 1.0 (see Results). This entry led to an exclusive formation of dimeric radical cations **2c/2e** but did not show any formation of formaldehyde. Although in **2c/2e** the alkoxide group is protonated whereas it is not as a result of reaction 27, this should not inhibit formation of an S∴O bond if it were favorable. This was confirmed in a separate experiment using 3,3′-DHP. Pulse irradiation of 3,3′-DHP at pH 6.9, i.e. under conditions where the alcohol group is well protonated, leads to an exclusive conversion of the hydroxyl radical adduct into the three-electron-bonded S∴O species **3**. Here the formation of the S∴O-bonded species is highly favorable through the five-membered-ring configuration.

It should be noted that the experiments carried out with 2-MTE and 2,2′-TDE at pH 1.0 indicate that also another possible pathway for the formation of alkoxy radicals **9c/9e**, namely, an electron-transfer process according to reaction 31, can also be ruled out. Species **2c/2e** are in equilibrium with their monomeric radical cationic forms, **12c/12e**, and should, in principle, undergo electron transfer if such a route were favorable.

In a second possibility formaldehyde might result from a *direct* abstraction of hydrogen from the alcoholic groups by hydroxyl radicals and subsequent α,β-fragmentation of the so-formed alkoxy radicals. Again radiolysis of 3,3′-DHP was used to invalidate this argument. The γ-irradiation of 3,3′-DHP solutions did not show any formation of formaldehyde at both pH values 1.0 and 6.5. The experiments with 3,3′-DHP underline the importance of six-membered hydrogen-bonded ring structures for the kinetics and product distribution in the hydroxyl radical induced oxidation of (alkylthio)ethanol derivatives. The 3,3′-DHP derivative permits the formation only of unfavorable seven-membered hydrogen-bonded ring structures. As a result the hydroxyl radical adduct at 3,3′-DHP does not undergo a fast

hydrogen-transfer process, finally leading to α-thioether radicals, but prefers the formation of the kinetically (and thermodynamically) more stable five-membered S.∴O-bonded ring structure.

Conclusion

The results from this study show the complexity by which reactive oxygen species, here the hydroxyl radical, undergo reactions with organic thioethers. The reaction of hydroxyl radicals with unsubstituted aliphatic alcohols occurs mainly under abstraction of α-hydroxyl hydrogen atoms and only negligibly (ca. 1%) via abstraction of hydroxyl hydrogens.[37] A somewhat reverse situation is observed for (alkylthio)ethanol derivatives where the main pathway involves formation of alkoxy radicals, enforced through beneficial conformational arrangements and the fact that the hydroxyl radical is trapped at the sulfur before any subsequent process can occur. We would like to point out that even more surprising results might be expected during the oxidation of thioethers (methionine) in peptides and proteins which provide a manifold of neighboring groups and the possibility of favorable conformational arrangements already before the attack of a free radical. Studies concerning oxidation of methionine in peptides and proteins by free radicals are currently under way and will benefit from the insight gained through investigations of the free radical induced oxidation of model compounds such as described in this paper.

(37) Asmus, K.-D.; Möckel, H.; Henglein, A. *J. Phys. Chem.* **1973**, *77*, 1218–1221.

Acknowledgment. The research described herein was supported by Hoffmann-LaRoche (Ch.S.) and by the Office of Basic Energy Sciences of the Department of Energy (K.B.). This is Contribution No. NDRL-3558 from the Notre Dame Radiation Laboratory. We would like especially to thank Professor R. L. Schowen for many helpful discussions and comments. One referee pointed out the possibility of formaldehyde formation through reactions 27–29. Although we think that this pathway is not a major pathway in our system, we would like to express our thanks for his valuable scientific advice.